21. Trends are least squares linear regression estimates. Confidence intervals are ±2 SD of the trend estimate, with the number of degrees of freedom adjusted for lag-one autocorrelation in the monthly anomaly time series.
22. A. Kattenberg *et al.*, in *Climate Change 1995: The Science of Climate Change*, J. T. Houghton *et al.*, Eds. (Cambridge Univ. Press, Cambridge, 1996), p. 285–357.
23. H. F. Diaz and N. E. Graham, *Nature* **383**, 152 (1996).
24. E. K. Roeckner *et al.*, *Report No. 93* (Max-Planck-Institut für Meteorologie, Hamburg, Germany, 1992).
25. Web table 1 is available at www.sciencemag.org/feature/data/1046022.shl.
26. L. G. Thompson *et al.*, *Global Planet. Change* **7**, 145 (1993); L. G. Thompson, *Quat. Sci. Rev.* **19**, 19 (2000).
27. P. Molnar and K. A. Emanuel, *J. Geophys. Res.* **104**, 24265 (1999).
28. P. H. Stone and J. H. Carlson, *J. Atmos. Sci.* **36**, 415 (1979).
29. For each sounding, layer mean surface-to-700-hPa lapse rates ($-\partial T/\partial Z$) were computed as $(T_{sfc} - T_{700})/(Z_{700} - Z_{sfc})$, where temperature T is the measured value at the surface and 700 hPa, Z_{700} is the geopotential height at 700 hPa, and Z_{sfc} is the surface elevation. Daily layer mean 700-to-500-hPa lapse rates were computed as $(T_{700} - T_{500})/(Z_{500} - Z_{700})$. Monthly means and quartiles were computed separately from 0000 and 1200 UTC soundings. Temporal increases in lapse rates mean a steepening of the rate of decrease of T with Z and a tendency toward more unstable conditions.
30. Empirical orthogonal function analysis of the data reveals strong spatial consistency of the lapse-rate trends. The dominant mode of variability, which explains 21% of the total variance, has a spatial pattern that is positive throughout the domain and a temporal structure showing an increase from 1979 to 1997.
31. D. S. Gutzler [*J. Atmos. Sci.* **53**, 2773 (1996)] found increasing instability at four tropical west Pacific radiosonde stations. Potential temperature differences between 300 and 1000 hPa increased during 1973–93 in association with increases in lower tropospheric water vapor.
32. R. J. Stouffer, G. C. Hegerl, S. F. B. Tett, *J. Clim.*, **13**, 517 (2000).
33. B. D. Santer *et al.*, *Science* **287**, 1227 (2000).
34. The three coupled ocean-atmosphere models are the Parallel Climate Model (PCM), the Climate System Model (CSM), and Max-Planck-Institut für Meteorologie ECHAM4/OPYC model. Based on the distributions of lapse-rate trend values in each model run, Fig. 2C shows the ranges, encompassing 95% of the distribution. Monthly layer mean lapse rates were computed in the same manner as the observations, but with monthly mean temperatures and heights at 700 hPa, 2-m (surface) air temperature, and the models' surface elevation. L. Bengtsson, E. Roeckner, and M. Stendel (*15*) discuss the ECHAM4 model; B. A. Boville and P. R. Gent [*J. Clim.* **11**, 1115 (1998)] describe the CSM; and the PCM is discussed by W. M. Washington *et al.* (*Clim. Dyn.*, in press).
35. We are grateful to L. Bengtsson, E. Roeckner, and M. Esch (Max-Planck-Institut für Meteorologie) for supplying the ECHAM3 model and the ECHAM4/OPYC simulations; T. Wigley [National Center for Atmospheric Research (NCAR)] for the CSM simulations; G. Meehl (NCAR) for the PCM simulations; M. Tyree (Scripps Institution of Oceanography) for performing ECHAM3 model runs; and J. Angell and M. Free (NOAA) for beneficial discussions.

5 October 1999; accepted 29 December 1999

Self-Assembling Amphiphilic Siderophores from Marine Bacteria

J. S. Martinez,[1] G. P. Zhang,[1] P. D. Holt,[1] H.-T. Jung,[2] C. J. Carrano,[3] M. G. Haygood,[4] Alison Butler[1]*

Most aerobic bacteria secrete siderophores to facilitate iron acquisition. Two families of siderophores were isolated from strains belonging to two different genera of marine bacteria. The aquachelins, from *Halomonas aquamarina* strain DS40M3, and the marinobactins, from *Marinobacter* sp. strains DS40M6 and DS40M8, each contain a unique peptidic head group that coordinates iron(III) and an appendage of one of a series of fatty acid moieties. These siderophores have low critical micelle concentrations (CMCs). In the absence of iron, the marinobactins are present as micelles at concentrations exceeding their CMC; upon addition of iron(III), the micelles undergo a spontaneous phase change to form vesicles. These observations suggest that unique iron acquisition mechanisms may have evolved in marine bacteria.

Low iron concentrations in surface seawater [typically from 20 pM to 1 nM (*1*)] limit primary production by phytoplankton in regions characterized by high concentrations of nitrate and other nutrients but low concentrations of chlorophyll (HNLC, high nitrate low chlorophyll) (*2*). In addition to phytoplankton and cyanobacteria, heterotrophic bacteria make up an important class of microorganisms in the ocean that are also limited by low iron levels in HNLC regions (*3–5*). Heterotrophic bacteria constitute up to half of the total particulate organic carbon in ocean waters (*4*), and in some regions, such as the subarctic Pacific, heterotrophic bacteria can even contain higher cellular concentrations of iron than phytoplankton (*5*). Heterotrophic bacteria thus compete successfully for iron against phytoplankton and cyanophytes and play a substantial role in the biogeochemical cycling of iron in the ocean. However, little is known about the molecular mechanisms used by marine bacteria, in particular, and other marine microorganisms, in general, to sequester iron. Marine bacteria are known to produce siderophores (*6–8*), which are low–molecular weight compounds secreted to scavenge Fe(III) from the environment and to facilitate its uptake into microbial cells. We report herein the structures and properties of a class of self-assembling amphiphilic siderophores produced by marine bacteria. Two families of siderophores, produced by two different genera of bacteria, each contain a unique peptidic head group that coordinates Fe(III) and one of a series of fatty acid tails.

Three strains, designated DS40M3, DS40M6, and DS40M8, were isolated from the same sample of ocean water, which had been collected at a depth of 40 m over the continental slope in the eastern equatorial Atlantic (*7*). The aquachelin siderophores (Fig. 1), produced by *Halomonas aquamarina* DS40M3 (Fig. 2), and the marinobactin siderophores (Fig. 1), produced by *Marinobacter* species strains DS40M6 and DS40M8 (Fig. 2), were isolated and purified from the supernatant of bacterial cultures, as previously described (*7*). The amino acid composition of the aquachelins and marinobactins, including the enantiomeric configuration, was determined with Marfey's reagent [*N*-a-(2,4-dinitro-5-fluorophenyl)-L-alaninamide] (*9*). The amino acid sequence was established by tandem mass spectrometry (Fig. 1) and confirmed by nuclear magnetic resonance (NMR) spectroscopy (*10*). The position of the D- and L-amino acids was determined from amino acid analysis of partially hydrolyzed peptide fragments generated from the native siderophore (*11*). Elucidation of the fatty acid moieties involved gas chromatography–mass spectrometry comparison to standard methyl ester derivatives, ozonolysis to establish the position of the double bond, and NMR to elucidate the configuration of the double bond (*10*). The connectivity of diaminobutyric acid and β-hydroxyaspartic acid in the marinobactin ring was determined by NMR (*10*).

The only terrestrial siderophores that bear a structural resemblance to marinobactins and aquachelins are the mycobactins and exochelins produced by mycobacteria, such as *Mycobacterium tuberculosis*, which also usually contain a fatty acid tail (*12*, *13*). The exochelins and mycobactins share a common hydrophilic core that coordinates Fe(III), but they differ in the substitution and chain length of the fatty acid. The hydrophilic exochelins, which are secreted

[1]Department of Chemistry and Biochemistry, University of California, Santa Barbara, CA 93106–9510, USA. [2]Department of Chemical Engineering, University of California, Santa Barbara, CA 93106, USA. [3]Department of Chemistry, Southwest Texas State University, San Marcos, TX 78666, USA. [4]Marine Biology Research Division, Scripps Institution of Oceanography, University of California, San Diego, La Jolla, CA 92093–0202, USA.

*To whom correspondence should be addressed. E-mail: Butler@chem.ucsb.edu

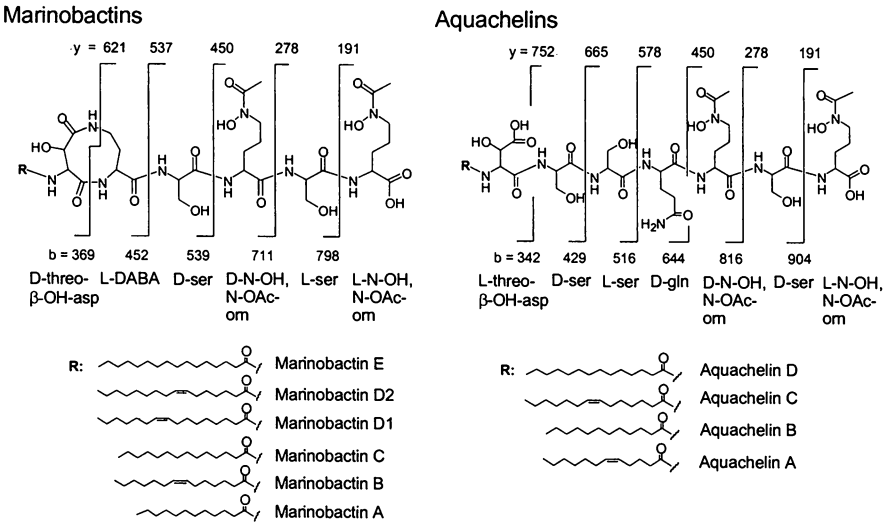

Fig. 1. The structures of the marinobactins and aquachelins. The vertical lines through the structures show the mass-to-charge ratio values for the y and b fragments obtained for marinobactin E and aquachelin D by tandem mass spectrometry. The "y" and "b" nomenclature refers to the charge when retained by the COOH-terminal fragment or the NH_2-terminal fragment of the peptide, respectively (*24*).

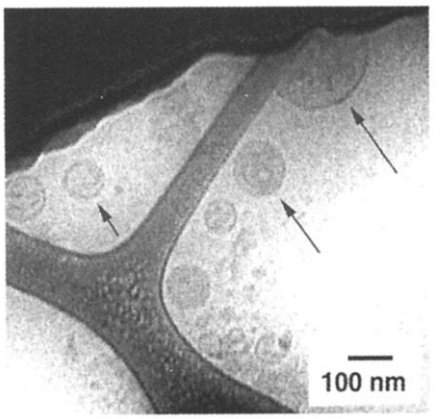

Fig. 3. Cryoelectron micrograph of Fe(III)–marinobactin D siderophore vesicles in aqueous solution. Representative vesicles are indicated by arrows. Samples were prepared for imaging by the method of Bellare *et al.* (*27*). The vesicles shown here result from 2 mM Fe(III)–marinobactins D in 100 mM tris-HCl (pH 8.0); the sample was rapidly frozen from a temperature of 25°C (*28*). The ratio of marinobactin D_2 to D_1 was about 3:1.

into the growth medium, have short alkyl side chains (C2-C8) and a terminal methylester moiety (*12*), whereas the mycobactins, which remain associated with the bacterium, have longer fatty acid groups (C16-C21) (*13*). The mycobacteria acquire iron by a shuttle system in which the secreted exochelins transport ferric ion to the membrane-associated mycobactins (*12*). However, it is clear that the iron acquisition process of mycobacteria differs fundamentally from that of *H. aquamarina* and the *Marinobacter* species. The marinobactins, aquachelins, and mycobactins have long fatty acid moieties, but only the marinobactins and aquachelins are secreted into the growth medium, and they are surprisingly hydrophilic. In addition, we find no evidence in the marine bacteria for cell membrane–associated siderophores, further illustrating the difference in iron uptake strategies of these bacteria.

The unique feature of the marinobactin and aquachelin siderophores, with their polar peptidic head groups and hydrophobic fatty acid tails, is their amphiphilic, surface-active nature, which leads to the formation of self-assembled structures. The iron-free marinobactins are characterized by unusually low critical micelle concentrations (CMC) ranging from 25 μM for marinobactin E to 150 μM for the shorter fatty acid chain lengths (*14*). The ferrated marinobactins also behave as surface-active agents, with slightly higher CMC values (*15*). Dynamic light-scattering results on a 0.2 mM solution of $[Fe(III)–marinobactin\ E]^-$ indicate the presence of spherical particles ranging in diameter from 140 to 180 nm (*16*), whereas the corresponding iron-free form of marinobactin E did not scatter light, suggesting that it is limited to micellar assembly. Similar results were obtained for aquachelins A and D. Cryoelectron microscopy on a 2 mM solution of the $[Fe(III)–marinobactins\ D]^-$ complex demonstrated the formation of polydisperse spherical vesicles ranging in size from 50 to 200 nm (Fig. 3). These vesicles spontaneously self-assemble in solution upon

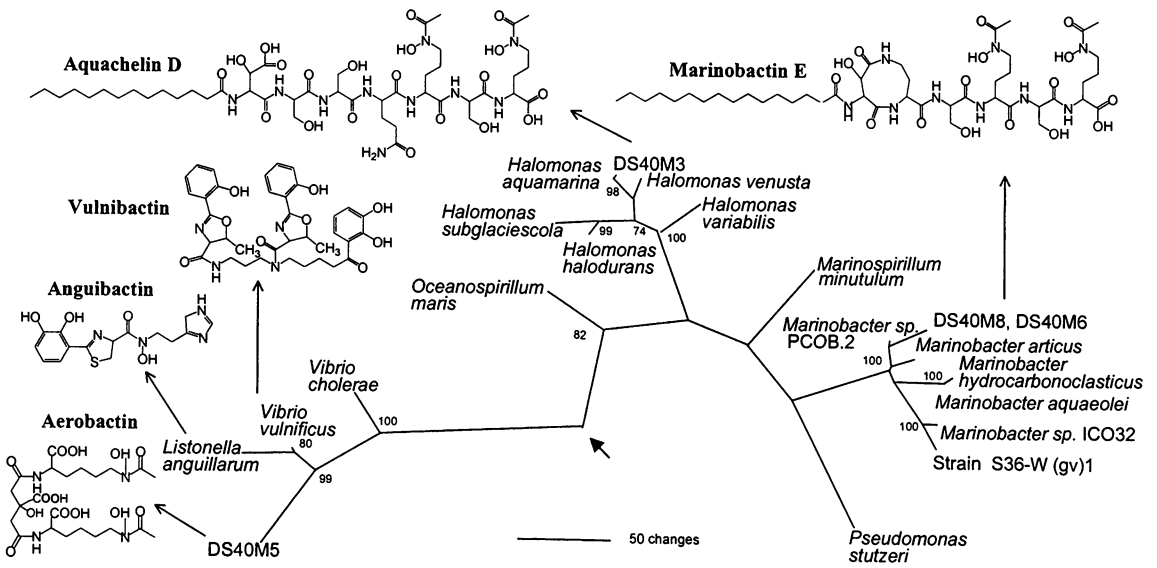

Fig. 2. Phylogenetic tree of marine proteobacteria based on maximum parsimony analysis of 16*S* rRNA gene sequences (*25*). The tree is one of eight best trees obtained by the branch and bound search algorithm. The eight trees vary only in the arrangement within the genera *Marinobacter* and *Halomonas*. Branch lengths are proportional to number of changes, with a transversion cost of two. Bootstrap support of greater than 70% is indicated next to nodes. The position of the outgroup (alpha proteobacterium *Agrobacterium tumefaciens*) is indicated by an arrow. In addition to aquachelin D and marinobactin E, the structures of aerobactin (*7*), vulnibactin (*8*), and anguibactin (*26*) are shown next to the marine bacterium from which they are produced.

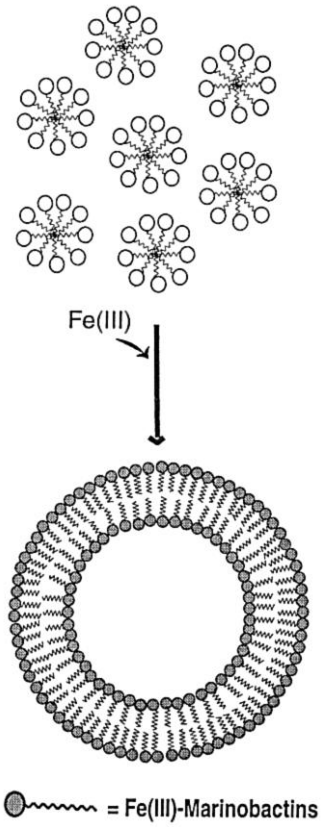

Fig. 4. Schematic representation of the phase change from a micellar assembly of the marinobactins in the absence of Fe(III) to vesicle formation upon coordination of Fe(III) to the siderophore. The relative head group size between micelle and vesicle is not drawn to scale.

addition of Fe(III) to the desferri form of the siderophore. The tendency of the free ligand to form micelles is not surprising, given that single-chain surfactants generally form micelles as a result of the large polar head group compared with the nonpolar tail, promoting a conically shaped molecule. As predicted, the transition from micelle to vesicle upon coordination of ferric ion is consistent with a more cylindrically shaped molecule (*17*).

The transformation from micelle to vesicle upon Fe(III) coordination (Fig. 4) is the first example, to our knowledge, of such a metal-induced phase change in a biologically produced compound. The presence of this metal-induced switch raises questions about the physiological role for this transformation. One potential physiological advantage of a micelle or vesicle structure, as opposed to a monomolecular species, might be protection from proteolytic cleavage, as has been recently demonstrated for synthetic lipopeptides (*18*). In fact, proteases and other degradative enzymes are widely dispersed in ocean water and even reside on the surface of pelagic marine bacteria (*19*). Although we would not expect micelles or vesicles to form in the low dissolved organic carbon and iron conditions of seawater, appropriate conditions might exist in particles or other microenvironments. These assemblies and the general lipophilic nature of the siderophores could represent a specific adaptation, perhaps for concentration of iron or for increasing the residence time in such habitats.

The aquachelins produced by *H. aquamarina* strain DS40M3 and the marinobactins produced by *Marinobacter* strains DS40M6 and DS40M8 are remarkably similar in that each has a peptidic head group that coordinates Fe(III) and a fatty acid tail, which confers the lipophilic properties to this class of siderophores. It is quite striking that these siderophores, whose distinctive properties hint at the possibility of a novel iron acquisition mechanism, are made by strains from two different genera within the gamma proteobacteria. Whether the structural strategy represented by these siderophores constitutes a specific adaptation to the seawater environment and whether it is widespread among marine bacteria are important questions for further studies.

References and Notes

1. K. W. Bruland, J. R. Donat, D. A. Hutchens, *Limnol. Oceanogr.* **36**, 1555 (1991); J. H. Martin, R. M. Gordon, S. E. Fitzwater, *Limnol. Oceanogr.* **36**, 1793 (1991); P. M. Saager, H. J. W. de Baar, P. H. Burkill, *Geochim. Cosmochim. Acta* **53**, 2259 (1989); J. Wu and G. W. Luther III, *Geochim. Cosmochim. Acta* **60**, 2729 (1996).
2. J. H. Martin *et al.*, *Nature* **371**, 123 (1994); K. H. Coale *et al.*, *Nature* **383**, 495 (1996), and references therein.
3. J. Granger and N. M. Price, *Limnol. Oceanogr.* **44**, 541 (1999); P. D. Tortell, M. T. Maldonado, J. Granger, N. M. Price, *FEMS Microbiol. Ecol.* **29**, 1 (1999).
4. J. D. Pakulski *et al.*, *Nature* **383**, 133 (1996).
5. P. D. Tortell, M. T. Maldonado, N. M. Price, *Nature* **383**, 330 (1996).
6. A. Butler, *Science* **281**, 207 (1998); D. A. Hutchins, A. E. Witter, A. Butler, G. W. Luther III, *Nature* **400**, 858 (1999); R. T. Reid, D. H. Live, D. J. Faulkner, A. Butler, *Nature* **366**, 455 (1993); C. G. Trick, *Curr. Microbiol.* **18**, 375 (1989); E. R. Goyne and E. J. Carpenter, *Limnol. Oceanogr.* **19**, 840 (1974); S. W. Wilhelm and C. G. Trick, *Limnol. Oceanogr.* **39**, 1974 (1994); S. W. Wilhelm, D. P. Maxwell, C. G. Trick, *Limnol. Oceanogr.* **41**, 89 (1996).
7. M. G. Haygood, P. D. Holt, A. Butler, *Limnol. Oceanogr.* **38**, 1091 (1993).
8. N. Okujo *et al.*, *Biometals* **7**, 109 (1994).
9. P. Marfey, *Carlsberg. Res. Commun.* **49**, 591 (1984).
10. The amino acid sequence was determined by nuclear Overhauser effect spectroscopy and heteronuclear multiple-bond correlation NMR, establishing the ^{1}H-^{13}C connectivities. The cis configuration of the double bond in the fatty acid residues was established by ^{1}H, ^{13}C, and heteronuclear quantum coherence NMR.
11. P. Demange, M. A. Abdallah, H. Frank, *J. Chromatogr.* **438**, 291 (1988).
12. J. Gobin and M. A. Horowitz, *J. Exp. Med.* **183**, 1527 (1996).
13. J. Gobin *et al.*, *Proc. Natl. Acad. Sci. U.S.A.* **92**, 5189 (1995).
14. Surface tension measurements were made with a Fisher Model 21 Tensiomat with a 5.99-IR loop and jacketed 20-ml cell thermostated at 25°C. The CMC value was estimated from the intersection of the extrapolated linear portions of the plot of surface tension versus siderophore concentration.
15. The CMC of desferri–marinobactin E at pH 3, at which the siderophore has no net charge, is 25 μM. Under these conditions, the CMC does not vary with ionic strength (for 0 to 1.0 M KCl). However, at pH 7.0, at which the head group bears a −1 charge due to deprotonation of the terminal carboxylate group, the related desferri–marinobactin D has an ionic strength–dependent CMC, ranging from 100 μM at 0 M KCl to 35 μM at 1.0 M KCl.
16. Dynamic light-scattering measurements were performed on Fe(III)-marinobactin vesicles prepared by addition of ferric nitrate to a solution of the desferri form of the marinobactins in 100 mM tris-HCl (pH 8.0). Scattered light from a 30-mW, 633-nm helium-neon laser at an angle of 90° was collected and analyzed with a Brookhaven Instruments BI-9000AT Digital Correlator to determine the effective diffusion constant of the vesicles, which was converted to hydrodynamic radius [D. F. Evans and H. Wennerstrom, *The Colloidal Domain* (VCH, New York, 1994)].
17. J. N. Israelachvili, S. Marcelja, R. G. Horn, *Q. Rev. Biophys.* **13**, 121 (1980).
18. K. C. Lee, P. A. Carlson, A. S. Goldstein, P. Yager, M. H. Gelb, *Langmuir* **15**, 5500 (1999).
19. F. Azam, *Science* **280**, 694 (1998).
20. D. S. Lane, in *Nucleic Acid Techniques in Bacterial Systematics*, E. Stackebrandt and M. Goodfellow, Eds. (Wiley, New York, 1990), pp. 115–148.
21. J. Brosius, T. J. Dull, D. D. Sleeter, H. F. Noller, *J. Mol. Biol.* **148**, 107 (1981).
22. B. L. Maidak *et al.*, *Nucleic Acids Res.* **27**, 171 (1999).
23. D. L. Swofford, PAUP*. Phylogenetic Analysis Using Parsimony (*and Other Methods). Version 4. (Sinauer Associates, Sunderland, MA, 1999).
24. P. Roepstorff, *Biomed. Mass Spectrom.* **11**, 601 (1989).
25. 16*S* ribosomal RNA (rRNA) sequences of marine siderophore producers (accession numbers AF199438, AF199439, and AF199440) were obtained from polymerase chain reaction products with standard primers (*20*). Both strands were sequenced, and the final sequences were aligned to the *E. coli* secondary structure (*21*). For phylogenetic analysis, sequences were obtained from the Ribosomal Database Project (RDP) (*22*) and GenBank and aligned with Sequencher. Accession numbers of sequences used for the analysis in Fig. 2 are M11223, U14584, M93352, L42619, M93358, M93357, L42618, X71814, AJ000726, AF148811, X67022, U85864, AJ000647, AB006769, U26262, X76334, and X74697. *Oceanospirillum maris* is an RDP sequence. Hypervariable regions were excluded, and a final data set of 1327 characters was analyzed with maximum parsimony in PAUP version 4.02b (*23*) with a transversion cost of two. Bootstrapping was done 1000 times with a heuristic search algorithm with 10 rounds of random addition at each replication. *H. aquamarina* and *H. meridiana* have indistinguishable 16*S* rRNA sequences, and the species status of *H. meridiana* is questionable. We compared phenotypic characters of the type strains of both species and strain DS40M3 and found the differences to be insignificant. Despite slight sequence differences between *H. aquamarina* and DS40M3, it is most conservative to regard it as a strain of *H. aquamarina*.
26. M. A. F. Jalal *et al.*, *J. Am. Chem. Soc.* **111**, 292 (1989).
27. J. R. Bellare, H. T. Davis, L. E. Scriven, Y. Talmon, *J. Electron Microsc. Tech.* **10**, 87 (1988).
28. The [Fe(III)-marinobactin]$^{-}$ vesicles are stable at 4°C for many months. They form and are stable under a variety of conditions, including artificial seawater and buffered solutions, with or without control of ionic strength.

29. Support from NIH grant GM38130 (A.B.), California Sea Grant (A.B.), NSF grant OCE 9633408 (M.G.H.), NSF grant CHE-9810248 under the Environmental Molecular Science Institute, CEBIC (Center for Environmental BioInorganic Chemistry) at Princeton University (A.B. and M.G.H.), and the NSF Material Science and Engineering Research Center program (for cryomicroscopy: J. Zasadzinski and H.-T.J.) is gratefully acknowledged. We also thank D. B. Edwards for sequencing, L. Xie for initial structure work, J. Pavlovich for mass spectrometry assistance, D. Live for NMR assistance, G. F. Xu and J. T. Groves for initial microscopy investigations and for insights into vesicle characterization, and C. Bewley, C. A. Burton, J. Cheetham, D. J. Faulkner, J. Israelachvili, D. J. Pine, and J. Zasadzinski for helpful discussions.

8 November 1999; accepted 21 December 1999